BBA - General Subjects 1861 (2017) 2342–2353

Contents lists available at ScienceDirect

BBA - General Subjects

journal homepage: www.elsevier.com/locate/bbagen

A new cryptic host defense peptide identified in human 11-hydroxysteroid dehydrogenase-1 β-like: from *in silico* identification to experimental evidence

A. Bosso[a,d,1], L. Pirone[b,1], R. Gaglione[c,d], K. Pane[a], A. Del Gatto[b], L. Zaccaro[b], S. Di Gaetano[b], D. Diana[b], R. Fattorusso[e], E. Pedone[b], V. Cafaro[a], H.P. Haagsman[d], A. van Dijk[d], M.R. Scheenstra[d], A. Zanfardino[a], O. Crescenzi[c], A. Arciello[c], M. Varcamonti[a], E.J.A. Veldhuizen[d], A. Di Donato[a], E. Notomista[a], E. Pizzo[a,*]

[a] *Department of Biology, University of Naples Federico II, 80126 Naples, Italy*
[b] *IBB, CNR, 80134 Naples, Italy*
[c] *Department of Chemical Sciences, University of Naples Federico II, 80126 Naples, Italy*
[d] *Department of Infectious Diseases and Immunology, Utrecht University, 3584 CS Utrecht, Holland*
[e] *Department of Environmental, Biological and Pharmaceutical Sciences and Technologies, University of Campania "Luigi Vanvitelli", I-81100 Caserta, Italy*

ABSTRACT

Background: Host defence peptides (HDPs) are evolutionarily conserved components of innate immunity. Human HDPs, produced by a variety of immune cells of hematopoietic and epithelial origin, are generally grouped into two families: beta structured defensins and variably-structured cathelicidins. We report the characterization of a very promising cryptic human HDP, here called GVF27, identified in 11-hydroxysteroid dehydrogenase-1 β-like protein.

Methods: Conformational analysis of GVF27 and its propensity to bind endotoxins were performed by NMR, Circular Dichroism, Fluorescence and Dynamic Light Scattering experiments. Crystal violet and WST-1 assays, ATP leakage measurement and colony counting procedures were used to investigate antimicrobial, anti-biofilm, cytotoxicity and hemolytic activities. Anti-inflammatory properties were evaluated by ELISA.

Results: GVF27 possesses significant antibacterial properties on planktonic cells and sessile bacteria forming biofilm, as well as promising dose dependent abilities to inhibit attachment or eradicate existing mature biofilm. It is unstructured in aqueous buffer, whereas it tends to assume a helical conformation in mimic membrane environments as well as it is able to bind lipopolysaccharide (LPS) and lipoteichoic acid (LTA). Notably it is not toxic towards human and murine cell lines and triggers a significant innate immune response by attenuating expression levels of pro-inflammatory interleukins and release of nitric oxide in LPS induced macrophages.

Conclusion: Human GVF27 may offer significant advantages as leads for the design of human-specific therapeutics.

General significance: Human cryptic host defence peptides are naturally no immunogenic and for this they are a real alternative for solving the lack of effective antibiotics to control bacterial infections.

1. Introduction

Antimicrobial peptides are natural multifunctional molecules produced by various organisms such as mammals, arthropods, plants and bacteria [1,2]. The largest group of antimicrobial peptides includes cationic antimicrobial peptides, also called host defense peptides

Abbreviations: HDP, host defence peptides; LPS, lipopolysaccharide; LTA, lipoteichoic acid; MIC, minimum inhibitory concentration; SD, standard deviation; CD, circular dichroism; TFE, trifluoroethanol; IL-6, interleukin 6; NO, nitric oxide; CFU, colony forming unit; RBC, red blood cell; HBTU, 2-(1H-benzotriazole-1-yl)-1,1,3,3-tetramethyluronium hexafluorophosphate; Oxyma, cyano-hydroxyimino-acetic acid ethyl ester; DIPEA, *N*,*N*′-diisopropylethylamine; TFA, trifluoroacetic acid; MeIm, 4-methylimidazole; MSNT, 1-(mesitylene-2-sulfonyl)-3-nitro-1,2,4-triazole; DMF, *N*,*N*-dimethylformamide; ACN, acetonitrile; DCM, dichloromethane; Fmoc, fluorenylmethyloxycarbonyl; CATH-2, cathelicidin-2; TSA, tryptic soy agar; AS, absolute score; MHB, Muller Hinton broth; NB, nutrient broth

* Corresponding author.
E-mail address: elipizzo@unina.it (E. Pizzo).
[1] Contributed equally.

http://dx.doi.org/10.1016/j.bbagen.2017.04.009
Received 25 December 2016; Received in revised form 5 April 2017; Accepted 24 April 2017
Available online 26 April 2017

(HDPs), effectors of the innate immune system that contribute to the rapid clearance of adverse biological agents [3]. In contrast to conventional antibiotics, HDP-mediated killing of microorganisms occurs via multiple mechanisms attacking both the cell membrane and/or intracellular targets [4]. Cationic HDPs have been proved to be active against virtually all types of existing pathogens which have shown none or poor ability to develop resistance to their antimicrobial activity [4,5]. In fact, it has been proposed that the resistance mechanisms would have high impacts on fitness and virulence of the mutants, since the pathogens need to acquire mutations on membrane and wall composition [6]. For this reason, current reports point out to the great potential of this class of innate immune molecules to constitute a novel group of wide spectrum therapeutic effectors.

Cationic HDPs are divided into subgroups on the basis of their amino acid composition and structure [7]: α-helical peptides, linear peptides enriched for specific amino acids (e.g. proline and arginine), and peptides containing cysteine residues and prone to form stable β-sheets. Cationic HDPs generally contain 12–50 amino acids, with 2–9 positively charged lysine or arginine residues, and up to 50% hydrophobic amino acids. They are able to interact with and insert into biomembranes on the basis of their hydrophobicity and net positive charge, conformational flexibility and secondary structure [8]. Additionally, many cationic HDPs can potentially prevent septic shock via their anti-endotoxic activity through electrostatic interactions with lipopolysaccharides (LPS) and lipoteichoic acid (LTA) in the bacterial membrane [9,10].

In addition to their antimicrobial activity, HDPs are able to modulate immune response, including the boosting of innate immunity and the suppression of inflammatory responses/endotoxaemia [11,12]. It has been noted indeed that some HDPs regulate LPS-induced gene transcription and cytokine production by several mechanisms as inhibition of LPS-induced translocation of the NF-kB subunits p50 and p65 [13], selective inhibition of gene transcription (e.g. p50, TNFAIP2) [13], reduction of the expression of others (TNF-α) [13], triggering of MAPK pathways that can impact on pro-inflammatory pathways [14], direct interaction with LPS to reduce its binding to LBP, MD2, or another component of the TLR4 receptor complex, thus reducing activation of the downstream pathway [15], and protection against the development of endotoxin shock *in vivo* [16]. Cationic HDPs may act either directly or indirectly, by selectively inducing chemokine production in immune cells and recruitment of other immune cells to the site of infection [17,18]. At the same time, HDPs may enhance antigen uptake and presentation and inhibit apoptosis of neutrophils and macrophages [17,18].

Cationic HDPs are expressed in different cell types, including monocyte/macrophages, neutrophils, epithelial cells, keratinocytes and mast cells. Some HDPs are constitutively expressed, whereas others are inducible by pathogen signature molecules, inflammatory conditions or tissue injury [19]. They are generally expressed as pro-peptides that undergo subsequent proteolytic processing to release the biologically active, mature host defense peptide [20].

It has been widely reported that in multicellular eukaryotes several proteins, with properties not necessarily associated to immunity, are sources of “cryptic” cationic host defense peptides [21]. These HDP releasing proteins release biologically active peptides only after their proteolytic processing by bacterial and/or host proteases.

The use of bioinformatic approaches has increased the possibility to highlight the presence of putative antimicrobial regions in proteins, thus representing an extremely useful tool for the discovery of new cryptic host defense peptides [22]. The bioinformatic strategy we recently developed [23] for the identification of potential HDP releasing proteins and the accurate localization of the fragment(s) hidden in their amino acidic sequences, is an example of such a procedure. The procedure we have developed is based on the finding that the antimicrobial potency (AP) of an HDP [defined as AP = Log(1000/MIC)] is linearly correlated to an “absolute score” (AS) which depends on charge, hydrophobicity and length of the peptide, and on two bacterial strain specific coefficients which determine the contribution of charge and hydrophobicity to the antimicrobial potency. Calculation of AS by a sliding window analysis provides a simple and effective method to localize HDPs (“cryptic” HDPs) contained within the structure of proteins, but also to analyze the internal structure of long HDPs, thus providing a very valuable tool for HDP identification and analysis.

Analyzing a pool of human secreted proteins using this approach, we identified a region rich in very high scoring peptides (see Fig. S1A and B) at the C-terminus of four isoforms of human 11-hydroxysteroid dehydrogenase-1 β-like (accession number UniProtKB: Q7Z5J1). It should be noted that human 11β-hydroxysteroid dehydrogenase type 1 (HSD 1) is a known NADP(H)-dependent enzyme that catalyzes the conversion of inactive glucocorticoids into active forms and its dysregulation is mainly implicated in the development of metabolic syndromes [24]. On the contrary, human 11-hydroxysteroid dehydrogenase-1 β-like, also known as 11-beta-hydroxysteroid dehydrogenase type 3 (HSD 3), the sequence in which the high scoring region has been found, has never been isolated as a protein and its membership to the hydroxysteroid dehydrogenase family has been assigned on the basis of the presence in the gene sequence of a putative dehydrogenase/reductase region partially similar to that extensively studied in HSD 1 [25]. The only type of evidence that supports the existence of HSD 3 as a protein is represented by expression data [26] that indicate the existence of a transcript (Gene ID: 374,875) apparently overexpressed in the brain and in lung cancer cells.

The isometric plot of the C-terminal region shows an absolute maximum (AS = 18.7 using the parameters determined for *S. aureus* C623) corresponding to a 39 residue long peptide (the longer arrow in Fig. S1A) and a local maximum (AS = 16.1) corresponding to a 26 residue long peptide (the shorter arrow in Fig. S1A). The region selected for the characterization (Fig. S1A and C), herein called GVF27, corresponds to this local maximum plus the glycine residue located upstream the 26 residues. The glycine residue was included in the peptide as, according to [27], a glycine at the N-terminus of an antimicrobial peptide is favorable for the activity.

In this work, we fully characterize peptide GVF27 describing its bactericidal properties against planktonic and sessile bacteria, its cytotoxic and anti-inflammatory effects on murine cells and its structural properties in the presence of mimic membrane agents and wall bacterial determinants, such as LPS and LTA.

2. Materials and methods

2.1. Peptide synthesis

Peptide GVF27 was manually synthesized using the fluorenylmethyloxycarbonyl (Fmoc) solid-phase strategy (0.1 mmol). Synthesis was performed on NovaSyn TGA resin (loading 0.25 mmol/g), using all standard amino acids. The first amino acid was bound to the resin by treatment with Fmoc-Thr(tBu)-OH (5equiv)/MSNT (5 equiv)/MeIm (3.75 equiv) in DCM for 3 h. Fmoc protecting group was removed by reaction with 30% piperidine in DMF (3 × 10 min). The amino acids in 10-fold excess were pre-activated with HBTU (9.8 equiv)/HOBT (9.8 equiv)/DIPEA (10 equiv) in DMF for 5 min and then added to the resin suspended in DMF. The reaction was carried out for 1 h and coupling efficiency was assessed by the Kaiser test. The peptide was cleaved off the resin by treatment with a mixture of trifluoroacetic acid (TFA)/water/triisopropylsilane (95:2.5:2.5 v/v/v) for 3 h at room temperature. Resin was filtered, and crude peptide was precipitated with diethyl ether, dissolved in H_2O/ACN solution, and lyophilized. The product was purified by preparative RP-HPLC on a Shimadzu system equipped with a UV − visible detector SPD10A using a Phenomenex Jupiter Proteo column (21.2 × 250 mm; 4 μm; 90 Å) and a linear gradient of H_2O (0.1% TFA)/ACN (0.1% TFA) from 20%–80% of ACN (0.1%TFA) in 20 min at a flow rate of 20 mL/min. Identity and purity of

the compound were assessed by LC/MS using an AGILENT Q-TOF LC/MS instrument equipped with a diode array detector combined with a dual ESI source and an Agilent C18 column (2.1 × 50 mm; 1.8 μm; 300 Å) at a flow rate of 200 μL/min and a linear gradient of H_2O (0.01% TFA)/ACN (0.01% TFA) from 5%–70% of ACN (0.01% TFA) in 15 min.

2.2. Antimicrobial activity assays

Antimicrobial activity of GVF27 peptide was tested against *Escherichia coli* ATCC 25922, MRSA WKZ-2 (methicillin-resistant *Staphylococcus aureus*), *Salmonella enteriditis* 706 RIVM, *Bacillus globigii* TNO BM013, *Bacillus licheniformis* ATCC 21424, *Staphylococcus aureus* ATCC 29213, *Pseudomonas aeruginosa* PAO1, and *Pseudomonas aeruginosa* ATCC 27853. Bacteria were grown to mid-logarithmic phase in Muller Hinton broth (MHB) at 37 °C. Cells were then diluted to 2×10^6 CFU/mL in Difco 0.5 × Nutrient Broth (Becton-Dickenson, Franklin Lakes, NJ) containing increasing amounts of GVF27 (0,6–40 μM). Starting from a peptide stock solution, two-fold serial dilutions were sequentially carried out, accordingly to broth microdilution method [28]. Following over-night incubation, MIC_{100} values were determined as the lowest peptide concentration responsible for no visible bacterial growth. Similar antimicrobial assays to test salt resistant properties of GVF27 have been carried out following the same procedure described above and using 0.5 × Nutrient Broth medium containing physiological concentrations of divalent cations as $CaCl_2$ and $MgSO_4$ (0.265 g/L and 0.097 g/L respectively).

2.3. Killing kinetics

To assess the time point of bacterial growth inhibition, killing kinetics with GVF27 were performed. Two different peptide concentrations (1 or 10 μM GVF27) were incubated with mid-logarithmic (2×10^6 CFU/mL) *E. coli* ATCC 25922 or MRSA WKZ-2. At 1, 5, 10, 20, 30, 60 and 120 min, 100 μL aliquots were taken and immediately plated on TSA. Additionally, 20 μL aliquots were diluted 10- to 1000-fold and again 100 μL was plated. After 16 h incubation at 37 °C the surviving bacteria were counted.

2.4. ATP leakage measurements

MRSA WKZ-2 and *Escherichia coli* ATCC 25922 were grown in Muller Hinton broth (MHB) at 37 °C to mid-logarithmic phase. Bacteria were centrifuged, resuspended in 10 mM phosphate buffer pH 7.0 + 1:100 MHB and diluted to 2×10^7 CFU/mL. From each diluted sample, 60 μL of bacterial suspension were incubated with 60 μL peptide solution (0.5 or 2 μM) for 5 min at 37 °C. Samples were then centrifuged, the supernatant was stored at 4 °C until further use, and the bacterial pellet was suspended in lysis buffer and further incubated at 100 °C. Cell lysates were centrifuged and supernatants were kept on ice. Subsequently, both intra- and extracellular ATP levels were determined using the Roche ATP bioluminescence kit HS II (Roche Diagnostics Nederland B.V., Almere, the Netherlands), according to the manufacturer's protocols.

2.5. Serum stability assays

The proteolytic susceptibility of GVF27 peptide was determined in 50% (v:v) human serum (Lonza, Basel, Switzerland). Human serum was previously activated by cooling at 4 °C, centrifugation at 13,000 × *g* for 5 min and incubation at 37 °C for 10 min in order to eliminate the lipid fraction. Then, 250 μL of serum was added to a 250 μL of an aqueous solution of GVF27 at a concentration of 1 mg/mL. The mixture was incubated at 37 °C and, after 1, 2, 3 and 24 h, samples (25 μL) were centrifuged at 13,000 × *g* for 5 min and the supernatant was added to 75 μL of H_2O containing 0.1% TFA and further centrifuged. Supernatants were finally analyzed by the analytical Agilent 1200 Series Liquid Chromatograph, equipped with a binary pump delivery system, robotic autosampler, column thermostat and multi-wavelength detector. An ET 250/8/4 Nucleosil 5-C18 column Machery-Nagel column (300 × 4 mm, 5 μm) and a linear gradient of H_2O (0.1%TFA)/CH_3CN (0.1%TFA) from 5 to 70% of CH_3CN (0.1%TFA) in 30 min at flow rate of 1 mL/min were employed. The experiment was run in duplicate.

2.6. Anti-biofilm activity assays

Escherichia coli strain ATCC 25922 was grown over-night in Muller Hinton broth (MHB) and then diluted to 1×10^8 CFU/mL in BM2 medium containing increasing peptide concentrations (0.125–32 μM). Incubation with the peptide was carried out either for 4 h, in order to test peptide effects on biofilm attachment, or for 24 h, in order to test peptide effects on biofilm formation. When peptide effects on preformed biofilm were evaluated, bacterial biofilms were formed for 24 h at 37 °C, and then treated with increasing concentrations of the peptide (0.125–32 μM). In all the cases, at the end of the incubation, the crystal violet assay [29] was performed. To do this, the planktonic culture was removed from the wells, which were washed three times with sterile PBS prior to staining with 0.04% crystal violet for 20 min. The colorant excess was eliminated by three successive washes with sterile PBS. Finally, the crystal violet was solubilized with 33% acetic acid and samples optical absorbance values were determined at 630 nm by using a microtiter plate reader (FLUOstar Omega, BMG LABTECH, Germany). To determine the percentage of viable bacterial cells inside the biofilm structure, upon biofilm disruption with 0,1% Triton X-100, bacterial cells were ten-fold diluted on solid TSA and incubated for 16 h at 37 °C. Once evaluated the number of colony forming units, bacterial cell survival was calculated as follows: $(CFU_{\text{in treated sample}} / CFU_{\text{in untreated sample}}) \times 100$.

2.7. Cytotoxicity assay

Cytotoxic effects of peptide on RAW 264.7 cells were determined using the cell proliferation reagent WST-1 (Roche Applied Science, Mannheim, Germany), designed to be used for the spectrophotometric quantification of cell proliferation. Briefly 5×10^4 cells were seeded into a 96-well plate and incubated at 37 °C with 5% CO_2. Medium was then replaced with 100 μL of fresh media containing peptide solution to a final concentration ranging from 0 to 40 μM/well. After 24 h of incubation at 37 °C, the peptide-containing medium was removed, and 100 μL of fresh medium containing 10% WST-1 reagent was added to each well and incubated for 30 min at 37 °C in the dark. Subsequently, the absorbance was measured in a microtiter plate reader (FLUOstar Omega, BMG labtech) at 450 nm, using 650 nm as the reference wavelength.

2.8. Hemolytic assay

EDTA anti-coagulated mouse blood was centrifuged for 10 min at 800 × *g* (20 °C) to sediment the red blood cells. Pelleted RBCs were washed three times and diluted 200-fold in PBS. In 96-well polypropylene plates, 75 μL of serial peptide dilutions (0–80 μM) were mixed with an equal volume of RBC suspension and incubated for 1 h at 37 °C. PBS served as baseline and a 0.2% (v/v) Triton X-100 solution served as a control for complete lysis. Supernatants, collected after 10 min centrifugation at 1300 × *g* (20 °C), were transferred into polystyrene 96-wells plates and absorbance was measured at 405 nm. Hemolysis (%) was calculated as follows: ((APeptide − ABlank) / (ATriton − ABlank)) × 100.

2.9. Measurement of nitric oxide production

Nitric oxide production was assessed as the accumulation of nitrite (NO_2^-) in cell supernatants as a result of 24 h incubation period. Nitrite concentrations were determined by a colorimetric reaction using the Griess reagent. Briefly, cell culture supernatants were mixed with an equal volume of 1% sulfanilamide (dissolved in 2.5% phosphoric acid) and incubated for 5 min. The same volume of 0.1% *N*-(1-naphthyl) ethylenediamine dihydrochloride was added and incubated for 5 min. The absorbance was measured at 520 nm using a 96-well microplate reader (FLUOstar Omega, BMG labtech).

2.10. Inhibition of IL-6 production mediated by GVF27

The ability of the peptide to modulate cytokine production in RAW 264.7 cells was measured by ELISA (enzyme-linked immunosorbent assay). Cells (5×10^4 cells/well) were seeded into 96-wells microtiter plates. The next day, culture medium was discarded and replaced with fresh medium either containing 1) a mixture of peptide (5 or 20 μM) and 50 ng/mL LPS (co-incubation) or 2) peptide alone (5 or 20 μM) for an initial incubation of 2 h followed by addition of 50 ng/mL LPS from *Salmonella* Minnesota (pre-incubation) or, 3) 50 ng/mL LPS for an initial incubation of 2 h followed by addition of peptide (5 or 20 μM, post-incubation). In all the cases, culture supernatants were collected after a total of 24 h incubation time. After each initial incubation with either LPS or peptide, the cells were washed three times with PBS prior to the subsequent addition of peptide or LPS to remove any residual traces of agents used during the pre-incubation. Expression levels of mouse IL-6 were measured using the commercial available DuoSet ELISA kits (R & D Systems), following the protocols provided by the manufacturer. All samples were centrifuged briefly at 5000 rpm for 3 min at room temperature to remove cell debris prior to use. Microtiter plates were read at 450 nm using 550 nm as a reference wavelength to correct optical imperfections of the microtiter plate.

2.11. LPS binding assay

The ability of GVF27 to neutralize LPS was determined using the commercially available Limulus amebocyte lysate (LAL) assay (Pierce® LAL Chromogenic Endotoxin Quantitation Kit, Thermo Scientific, USA) [30]. Briefly, 25 μL of serially diluted peptide (25,12.5, 6.25 μM) was added to 25 μL of 0.5 U/mL *E. coli* O11:B4 LPS for 30 min at 37 °C, followed by incubation with 50 μL of amoebocyte lysate reagent for 10 min. Absorbance at 405 nm was measured 10 min after the addition of 100 μL of the chromogenic substrate, Ac-Ile-Glu-Ala-Arg-p-nitroanilide. The amount of non-bound LPS was extrapolated from a standard curve, and percentage inhibition calculated as: [(amount of free LPS in control samples) − (amount of free LPS in test samples)] × 100 / amount of free LPS in control samples.

2.12. Spectroscopic studies

CD spectra of GVF27 were recorded with a J-810 spectropolarimeter equipped with a Peltier temperature control system (Model PTC-423-S, Jasco Europe, Cremella, LC, Italy). Far-UV measurements (190–260 nm) were carried out at 20 °C using a 0.1 cm optical path length cell and a peptide concentration of 25 μM. CD spectra were recorded as described elsewhere [31,32]. Baseline was corrected by subtracting the complete buffer spectrum. CD spectra were carried out in the presence of LPS from *Pseudomonas aeruginosa* strain 10 (Sigma, purified by phenol extraction) and from *P. aeruginosa* clinical strain KK27 (kindly provided by Prof. De Castro). Further analyses were carried out in the presence of lipotechoic acid from *Staphylococcus aureus* (LTA, Product Number L 2515, Sigma). All measurements were recorded using different concentration of each compound (from 0.05 to 1.0 mg/mL). Baseline was corrected by subtracting the spectrum of both LPS and LTA alone at the same concentration. Additional CD spectra were performed using different concentrations of trifluoroethanol (TFE) (0–40%). Deconvolutions of CD spectra were obtained using the web-based program CdPro (http://lamar.colostate.edu/~sreeram/CDPro/).

Fluorescence experiments were carried out under the same conditions used for CD analyses. Fluorescence spectra were collected at 20 °C using a Varian Cary Eclipse spectrophotometer at λ excitation of 295 and 280 nm, a 1.0 cm path length cell at 5 ε_{em} and 5 ε_{ex}. Emission spectra (300–400 nm) were collected in the presence of 40% TFE, 5 mg/mL LPS or 10 mg/mL LTA.

2.13. LPS micelles measurements by using Dynamic Light Scattering (DLS)

To estimate the average size of the LPS particles, the Hydrodynamic Radii (RH) was measured by Dynamic Light Scattering technique (DLS). DLS measurements were carried out using a Zetasizer Nano ZS (Malvern Instruments, Westborough, MA) equipped with a 173° backscatter detector, at 25 °C, using a disposable sizing cuvette. DLS measurements in triplicate were carried out on aqueous LPS and LTA samples at 0.5 mg/mL. Data were analyzed using the Software of OMNISIZE (Viscotek). LPS and LTA size measurements were performed before and after peptide addition (0.5 mg/mL).

2.14. Nuclear magnetic resonance spectroscopy

NMR experiments were recorded at 25 °C on a Varian Unity INOVA 600 MHz NMR spectrometer equipped with a cold probe. Two-dimensional (2D) nuclear Overhauser effect spectroscopy (NOESY), total correlation spectroscopy (TOCSY) and 2D double-quantum-filtered correlated spectroscopy (DQFCOSY) experiments were recorded [33]. NOESY mixing times were 200 ms and TOCSY mixing times were 70 ms. These experiments were collected with 512 and 1024 complex points with acquisition times of 64 and 128 ms in the indirectly and directly acquired 1H dimensions, respectively. The DQFCOSY experiment was collected with 1024 and 2048 complex points and acquisition times of 128 and 256 ms in the indirectly and directly acquired 1H dimensions, respectively. In all experiments water suppression was obtained using pre-saturation in order to simultaneously suppress the hydroxyl protons from TFE that are in fast exchange with protons from water. Hydroxyl protons from TFE were seen to attenuate signals in both 1D and 2D datasets in WATERGATE based suppression. 1D spectra were analyzed using ACD/NMR Processor 12.0 (ACD/NMR Processor Freeware, Version 12.01 Advanced Chemistry Development, Inc., Toronto, ON, Canada (2012), www.acdlabs.com). 2D TOCSY and NOESY spectra for 1H chemical shift assignment were analyzed using Neasy, a tool available in CARA (Computer Aided Resonance Assignment) software (Keller, R. L. J. The Computer Aided Resonance Assignment Tutorial. CANTINA Verlag, 2004, downloaded from cara.nmr.ch). Structure calculation was performed with the program CYANA version 2.1 [34]. The NOE cross peak intensities were used to obtain distance constraints. The angle restraints were derived from 3JHNHα coupling constants. Structure calculations were initiated from 100 random conformers; the 20 structures with the lowest CYANA target function ns were analyzed with the programs MOLMOL [35] and PyMOL Molecular Graphics System, Version 1.8 Schrödinger, LLC. (http://www.pymol.org/).

2.15. Statistics

Results are presented as the mean ± standard error of the mean (SEM) of at least three independent experiments. Statistical significance was assessed using one-way ANOVA in Prism software, version 6.02 (GraphPad Prism, La Jolla, CA, USA). All samples were compared to the negative control. *$p < 0.05$; **$p < 0.01$; ***$p < 0.001$.

Table 1
Minimum inhibitory concentration (MIC, μM) values of GVF27 peptide, compared to those obtained for chicken cathelicidin-2 (CATH-2), against a panel of Gram-positive and Gram-negative bacteria. Values were obtained from a minimum of three independent trials.

Gram positive strains	GVF27 MIC values (μM)	CATH-2	Gram negative strains	GVF27 MIC values (μM)	CATH-2
MRSA WKZ-2	5	10	*E. coli* ATCC 25922	10	10
B. globigii TNO BMO13	5	5	*P. aeruginosa* ATCC 27853	10	10
B. licheniformis ATCC 21424	5	20	*P. aeruginosa* PAO1	20	20
S. aureus ATCC 29213	5	10	*S. enteriditis* 706 RIVM	10	10

3. Results

3.1. Antibacterial activity

The antibacterial effectiveness of synthetic GVF27 (see Materials and methods section) was determined by measuring its MIC values on a panel of Gram-negative and Gram-positive strains (Table 1). All GVF27 MIC values are comparable to those observed for control peptide CATH-2 [36,37] both on Gram-negative and Gram-positive strains (Table 1). In order to verify salt resistant properties of GVF27, MIC values were determined also in the presence of physiological amounts of divalent cations (see Materials and methods section). As shown in Table S1, MIC values determined in the presence of divalent cations were practically identical to those obtained in NB (see Table 1 and S1), thus indicating that antimicrobial properties of GVF27 are not affected by the different experimental conditions tested. When the killing rate of GVF27 was measured, none of the strains analyzed (MRSA WKZ-2 and *E. coli* ATCC 25922) survived after 2 h at 10 μM peptide doses (see Fig. S2).

One of the mechanisms through which HDPs kill bacterial cells is by forming pores into biological membranes, resulting in the leakage of small molecules [38,39]. We tried to collect data on the mechanism of the antibacterial activity of GVF27 by measuring ATP levels in the media in which bacterial cells are grown in the presence of the peptide. In fact, in bacterial cells intracellular ATP concentration is maintained constant and the release of ATP into the environment can be detected by chemiluminescence, which indicates the disruption of the cell membrane. Thus, we performed an assay to detect ATP leakage using two bacterial strains, *E. coli* and MRSA, treated with two different doses of GVF27 for 20 min (see Materials and methods section). As shown in Fig. 1 (panels A and B), the presence of ATP in the culture media is evident. Thus, we can confidently conclude that GVF27 has a lytic effect both on MRSA WKZ-2 and on *E. coli* cells, with MRSA WKZ-2 cells being particularly sensitive to the peptide. As it is shown in Fig. 1, GVF27 induced in MRSA WKZ-2 cells a release of 70% ATP at a concentration of 0.5 μM. To obtain the same degree of ATP leakage in *E. coli* cells it was necessary a higher concentration of GVF27.

Bacteria mainly exist as multicellular aggregates embedded within a self-produced extracellular polymeric matrix. In this condition, known as biofilm, growing microbial cells are physiologically distinct from planktonic cells. As natural HDPs have emerged as promising anti biofilm candidates to be used as an alternative to conventional antibiotics, we evaluated if GVF27 is endowed with anti-biofilm activity by performing experiments on *E. coli* ATCC 25922 in BM2 medium. *E. coli* was grown over-night, diluted in BM2 medium containing increasing concentrations of the peptide (from 0,125 to 32 μM), and then incubated for 24 h, at 37 °C. Following incubation, the analysis of biofilm production by crystal violet staining revealed a dose-dependent inhibition of biofilm formation, with about 90% inhibition at the highest concentration of peptide tested (Fig. 2A). We also collected data that would indicate that GVF27 peptide exerts a significant effect on biofilm attachment. To investigate this, we followed the experimental procedure described above with the only exception that bacterial cells were incubated with increasing concentrations of peptide for 4 h, at 37 °C. Also in this case, we observed a dose-dependent inhibition of biofilm attachment, with almost total inhibition at 32 μM peptide concentration (Fig. 2A). Interestingly, GVF27 was found to exert significant effects also on preformed biofilms. This was evaluated by incubating preformed biofilm (see Materials and methods section) with increasing concentrations of the peptide for 24 h, at 37 °C. At the highest peptide concentration tested, we observed a significant (~ 20%) reduction of the preformed biofilm (Fig. 2A).

In all cases, we also evaluated the percentage of viable bacterial cells inside the biofilm by colony counting assay. We found (Fig. 2B) an almost total reduction of bacterial viability when 32 μM GVF27 was added prior to biofilm attachment, a significant reduction (90%) when it was added prior to biofilm formation and a reduction of about 50% when the peptide was tested on pre-formed biofilm.

3.2. Cytotoxicity assays of GVF27 on eukaryotic cells

As already reported [38,39], the promising interest in the use of HDPs stems from their selective action on bacterial cells. We thus

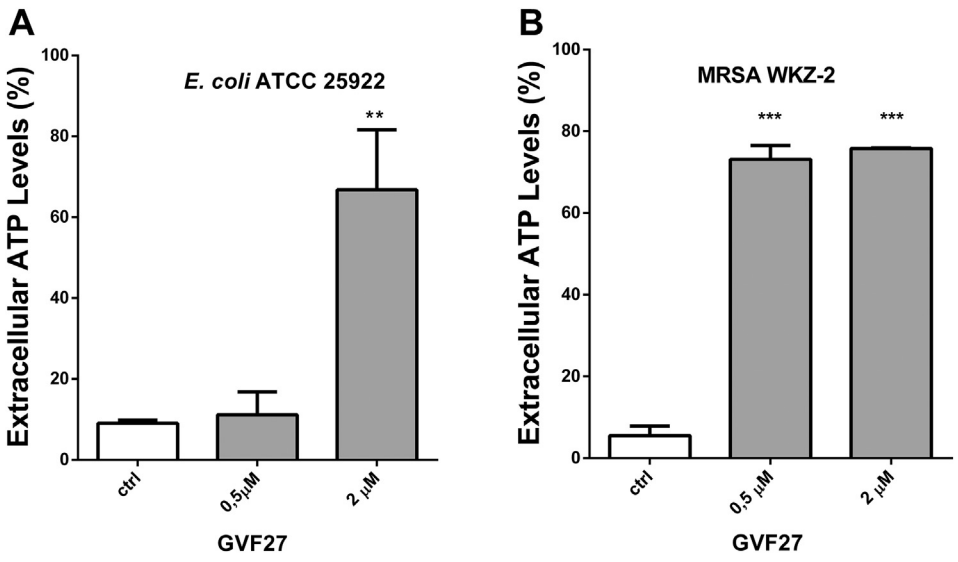

Fig. 1. GVF27-induced ATP leakage in *Escherichia coli* ATCC 25922 (A) and MRSA WKZ-2 (B) after treatment with 0.5 or 2 μM GVF27. The assays were performed in three independent experiments.

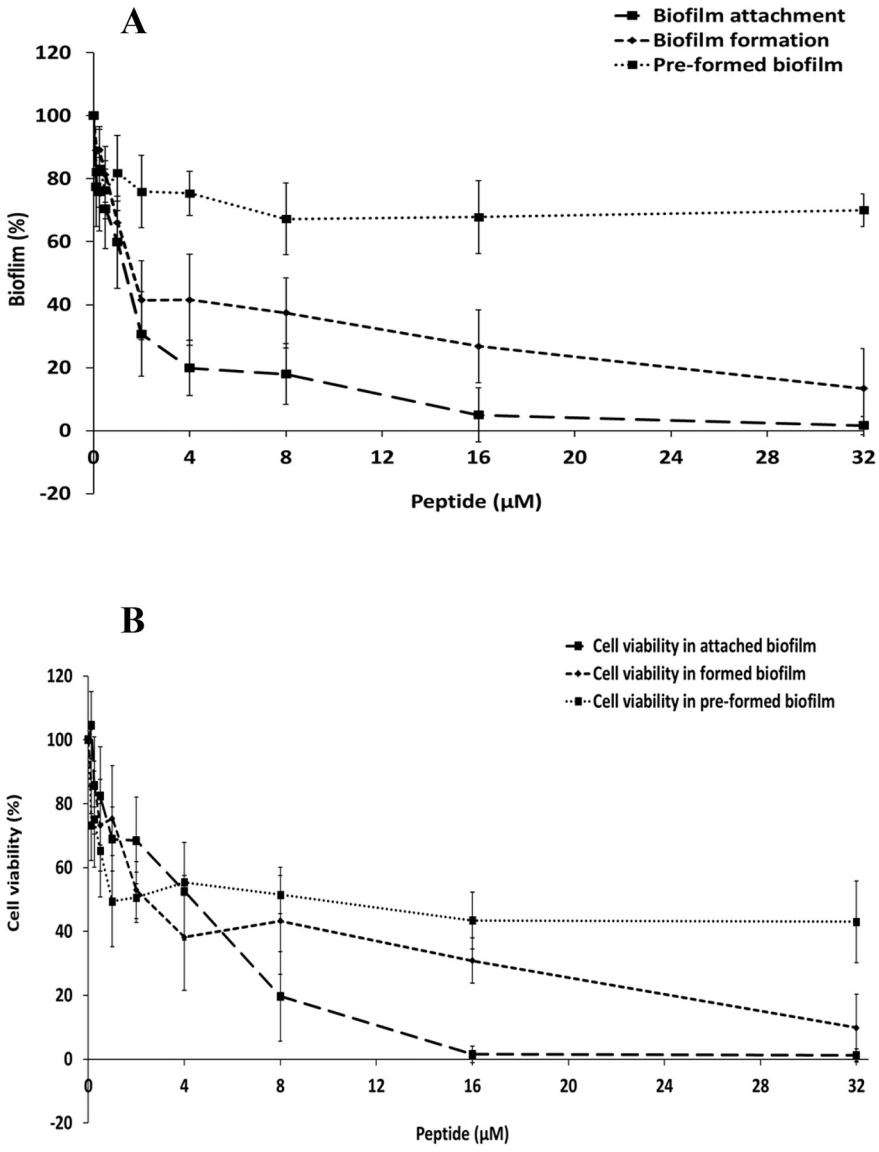

Fig. 2. A. Biofilm inhibitory activity of GVF27 against *E. coli* strain in BM2 medium. The effects of increasing concentrations of GVF27 peptide were evaluated either on biofilm formation, biofilm attachment, or on pre-formed biofilm. Biofilm was stained with crystal violet and measured at 630 nm. Shown are mean + SD values of three independent experiments. B. Effects of increasing concentrations of GVF27 peptide on the viability of *E. coli* ATCC 25922 bacterial cells inside the biofilm structure. Cell viability was assessed by colony counting assay and expressed as the percentage of viable bacterial cells in treated samples with respect to the control untreated sample. Shown are mean + SD values of three independent experiments.

studied the cytotoxic effect of GVF27 towards mouse macrophages and erythrocytes. The addition of increasing concentrations (from 0.6 to 40 μM) of GVF27 to mouse macrophages RAW 264.7 cells for 24 h did not result, in any significant reduction in cell viability (Fig. S3A). The same peptide concentrations were tested also on mouse erythrocytes to detect any hemolytic activity of GVF27. As shown in Fig. S3B, the peptide did not exert any lytic effect on mouse red blood cells, even at the highest concentration tested. The cytotoxicity of GVF27 was also measured against human keratinocytes (HaCat) and on human cervical cancer cells (HeLa). In all cases, no significant cytotoxicity was ever observed (data not shown). It should be underlined that GVF27 is toxic to bacterial cells (Table 1, Figs. S2, 1 and 2) at concentrations similar to that used in the cytotoxicity assays described above. Moreover, it should be noted that all the experiments mentioned above were carried out after an incubation time of 24 h, since the analysis of GVF27 stability in serum (see Materials and methods section) indicated that peptide degradation was almost complete after 24 h (see Table S2).

3.3. Conformational studies of GVF27

3.3.1. Circular Dichroism and Fluorescence

Structural analysis by CD spectroscopy provides a qualitative picture of the structural elements that are present in a given peptide. Far-UV CD spectra indicate that GVF27 is largely unstructured both in water and in 10 mM Hepes pH 7.4. On the contrary, it is structured in 40% TFE (Fig. 3). This behavior can be observed also for other HDPs [40,41], all prone to assume a specific conformation when interacting with membrane-mimicking agents like TFE. Moreover, deconvolution data (see Materials and methods section) reported in Table 2, indicate that structured GVF27 adopts a predominant helical structure (approximately of ≈ 50%).

To further characterize structural properties of GVF27, the interaction with LPS and LTA, the main constituents of the cell wall of Gram negative and positive bacteria, respectively, was analyzed. CD spectra in the presence of LPS isolated from two different *P. aeruginosa* strains (strain 10 and clinical isolate KK27 strain) are shown in Fig. 4 (panels A and B).

GVF27 spectrum in water has a minimum at around 205 nm, indicating that the peptide is in a disordered conformation. Instead, in the presence of LPS (Fig. 4A–B), the peptide spectra present two minima centered around 210 and 225 nm, suggesting that in both cases it is able to assume a helical conformation upon interaction. The deconvolution data (Table 2) confirm that both LPSs induce a similar increase in the amount of helical structure (about 31–32%) but with slightly different amounts of beta and coil structure.

CD spectra, acquired in the presence of LTA, (Fig. 4C), showed a

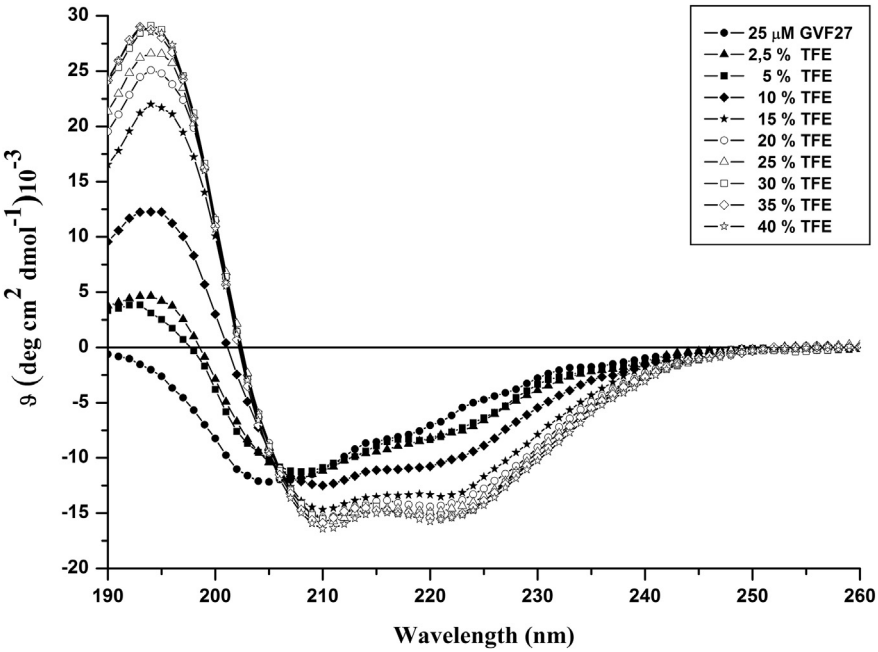

Fig. 3. Far UV CD of GVF27 in the presence of increasing concentrations of TFE.

Table 2
Secondary structure content of GVF27, calculated by means of CDPRO program.

	% α-helical	% β-strand	% coil
GVF27	**18.2**	**24.0**	**57.8**
GVF27 - 40 %TFE	**52.6**	**7.2**	**40.2**
GVF27 - 0,4 mg/mL LPS from *Pseudomonas aeruginosa* strain 10	**30.8**	**18.6**	**50.6**
GVF27 - 0,4 mg/mL LPS from *Pseudomonas aeruginosa* strain KK27	**32.1**	**12.3**	**55.5**
GVF27 - LTA 0,4 mg/mL	**33.0**	**19.5**	**47.5**

relatively flat shape minimum centered at 215 nm, due to the presence of significant amounts both of alpha and beta structures as shown by deconvolution data (Table 2).

Spectrofluorimetric data were also collected to investigate if the interaction of GVF27 with LPS and LTA could influence the tertiary structure of the peptide based on the presence in the sequence of three Trp residues (see Fig. S1). Fluorescence spectra were recorded upon excitation at 280 nm and 295 nm and showed (see Fig. S4) that the interaction of the peptide with LPS, LTA, and TFE results in a blue shift of the wavelength of the maximum of emission, indicating that GVF27 folds upon interaction with LPS or LTA, in agreement with CD data. However, in the presence of TFE a less marked effect was observed.

3.3.2. Structural characterization by NMR

A deeper investigation of the conformational preferences of peptide GVF27 was performed by NMR spectroscopy. In order to investigate the influence of the environment experienced by a membrane-interacting peptide on the structure, the NMR study was carried out both in bulk water, simulating the transport fluid, and in 30% TFE-d3/H2O) 30:70 (v/v) mixture, which reduces solvent polarity. The comparison of 1D spectra under these two conditions, reported in Fig. 5A (upper and lower trace for water and TFE/water mixture respectively) reveals that in the less polar environment the dispersion of the chemical shift is higher. This is confirmed by the comparison of the 2D NOESY spectra, reported in the panel B and C respectively, showing also a higher number of cross-peaks in the presence of TFE. Then, NMR characterization of GVF27 was performed in TFE-d3/H_2O 30:70 (v/v) mixture at 298 K. The standard sequential assignment approach based on homonuclear 2D 1H NMR [42] allowed the complete sequence specific ^{1}H NMR assignment (Table 3). Particularly, identification of spin systems and resonance assignment were established by a combination of two-dimensional DQF-COSY and TOCSY spectra, whereas sequence-specific assignment was obtained by NOESY experiments.

The values of the deviation of Hα chemical shifts (ΔδHα) analysis performed by using Chemical Shift Index (CSI) (Fig. S5) [43] and the ^{3}JHN-Hα couplings (Fig. S6) indicate the presence of a random coil structure in aqueous solution. On the other hand, GVF27 shows a significant change in the ^{1}H chemical shifts and in ^{3}JHN-Hα coupling values when TFE is added, suggesting that the entire polypeptide chain is involved in a conformational transition. Indeed, the ΔδHα and the ^{3}JHN-Hα coupling values indicate a high helical propensity of the entire polypeptide chain. Further, the 2D [^{1}H, ^{1}H] NOESY analysis showed several HN–HN (i, i + 1), Hα–HN (i, i + 3), and Hα–Hβ (i, i + 3) connectivities (see Fig. S7), confirming the presence of a helical conformation, in agreement with the trend suggested by the CSI analysis based on Hα and with CD data.

A set of 267 (119 intra-residual, 88 sequential and 66 medium and long-range) experimental NOE constraints (Table 4) was used as upper limits of inter-proton distances for structure calculations by CYANA program [34]. The backbone overlay of the best 20 CYANA conformers displays a good convergence confirmed by a backbone and all heavy atoms root-mean-square difference (rmsd) values of 0.19 ± 0.10 Å and 1.24 ± 0.15 Å respectively (Fig. 6). Apart from some dynamic fraying at the N-terminus, the calculated structures comprise a regular α-helix, in agreement with the NOE data, H-bonding (Table 5) and the pattern of φ/ψangles (Fig. S7).

3.4. GVF27 assembles LPS aggregates

DLS is a well-known technique used to measure Brownian motion (diffusion) and size distribution of particles in solution. For this reason DLS experiments were used to investigate whether peptide GVF27 may alter the size of micelles of LPS and LTA (above their critical micelle concentration). In both cases GVF27 displayed an associating action, promoting the formation of larger aggregates. In particular, the data indicate that LPS from *Pseudomonas* is poly-dispersed in solution with

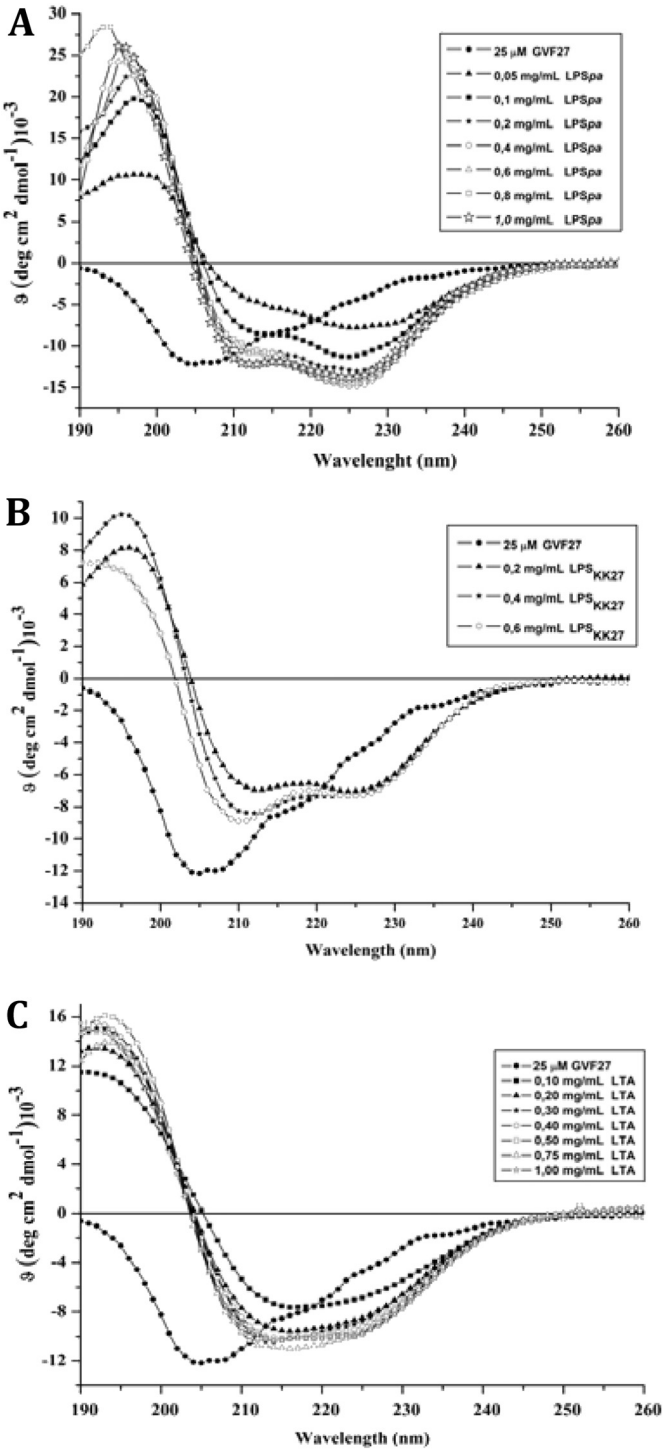

Fig. 4. Far UV CD of GVF27 in the presence of increasing concentrations of LPS from *P. aeruginosa* 10 (A), from *P. aeruginosa* KK27 (B) and of LTA from *Staphylococcus aureus* (C).

major size-populations having a hydrodynamic radius centered at about 40 nm (Fig. 7). Incubation of LPS with GVF27 causes a shift of the average size of LPS micelles to a higher value centered at about 260 nm. On the other hand, when the peptide was incubated with LTA, a mean diameter of 100 nm of the aggregates was observed, indicating a weaker potency of GVF27 in associating LTA aggregates.

It can be hypothesized that this aggregation action, already observed for other antimicrobial peptides [44], may be part of a LPS neutralization mechanism, inhibiting the interaction of LPS with its cell receptors, with the concomitant blocking of cytokine production and release [45].

3.5. Anti-inflammatory properties of GVF27

Data above would indicate that GVF27 is able to assume specific conformations in the presence of mimic membrane agents, LPS and LTA, as well as to induce aggregation of LPS, and to a lesser extent of LTA. As it is has been already reported that several HDPs are able to mitigate up-regulation of LPS-induced pro-inflammatory mediators and cytokines [7,46,47], it seemed interesting to verify if GVF27 could possess also putative anti-inflammatory properties. To collect data on possible anti-inflammatory properties of GVF27, nitric oxide production and interleukin Il-6 release by murine macrophages RAW 264.7 treated with GVF27 and LPS were analyzed.

Nitric oxide (NO) plays diverse roles in biological systems: it is a mediator of vasodilatation, platelet aggregation and neurotransmission, and regulates function, death and survival of various cell types including many of those involved in immunity and inflammation [48,49].

To study the effect of GVF27 on NO production in LPS activated RAW 264.7 cells, we performed three types of treatments: 1. medium containing a mixture of peptide (5 or 20 μM) and 50 ng/mL LPS; medium containing peptide alone (5 or 20 μM) for an initial incubation of 2 h followed by addition of 50 ng/mL LPS from *Salmonella* Minnesota; 2. medium containing 50 ng/mL LPS for an initial incubation of 2 h followed by addition of peptide (5 or 20 μM). In all the cases, culture supernatants were collected after 24 h. As shown in Fig. 8A, GVF27 exerts a strong dose-dependent attenuation of the production of NO when co-incubated with 50 ng/mL LPS. Conversely, when we performed a pre-incubation of RAW 264.7 cells with peptide and subsequently we induced LPS stimulation, the effect of GVF27 on NO production was not significant (Fig. 8A). Similarly, when RAW 264.7 cells were pre-incubated with LPS and subsequently treated with 5 or 20 μM of GVF27, we revealed a slight dose dependent reduction of NO production (Fig. 8A).

Cytokines are small proteins (about 25 kDa) released by many cell types, usually after an activation signal, and they induce a response by binding specific receptors. IL-6 is a monomer produced by T cells, macrophages and endothelial cells. It is able to determine growth and differentiation of B and T cells, and the production of acute phase proteins, like C-reactive protein [50].

When we analyzed the effect of GVF27 on RAW 264.7 cells by ELISA (see Materials and methods section), following the same scheme used in the NO production assay, we revealed a strong inhibitory effect exerted by the peptide on the secretion of IL-6 when the macrophages were co-incubated for 24 h with GVF27 (5 or 20 μM) and 50 ng/mL LPS (see Fig. 8B). Moreover, we found that GVF27 was also able to exert a significant dose dependent protective effect on cells. Indeed, as shown in Fig. 8B (on the center), when RAW 264.7 cells were pre-treated for two hours with 5 or 20 μM GVF27 and then incubated for an additional 22 h with 50 ng/mL LPS, we observed a reduction of the IL-6 secretion, indicating a prolonged peptide effect. When cells, were pre-incubated with LPS and then subjected to the action of the peptide (see Fig. 8B – on the right), still we were able to observe a reduction in IL-6 secretion, although the LPS-induced secretion itself was already low due to the very short LPS incubation time in this set-up Collectively, these data indicate that GVF27 is able to exert an intriguing anti-inflammatory effect on LPS treated cells.

Finally, the ability of GVF27 to bind LPS, was further confirmed by a different approach using the chromogenic LAL (*Limulus amaebocyte* lysate) assay [51] Three different concentrations of GVF27 (6.25–12.5–25 μM) were incubated for 30 min at 37 °C with LPS from *Escherichia coli* 011:B4 following manufacturer instructions. As shown in Fig. S8, a concentration of 12.5 μM GVF27 was enough to neutralize about 40% of LPS whereas the presence of 25 μM GVF27 completely neutralized LPS thus supporting the hypothesis that GVF27 might act in a dose-dependent manner as a scavenger of Gram negative's LPS (Fig. S8).

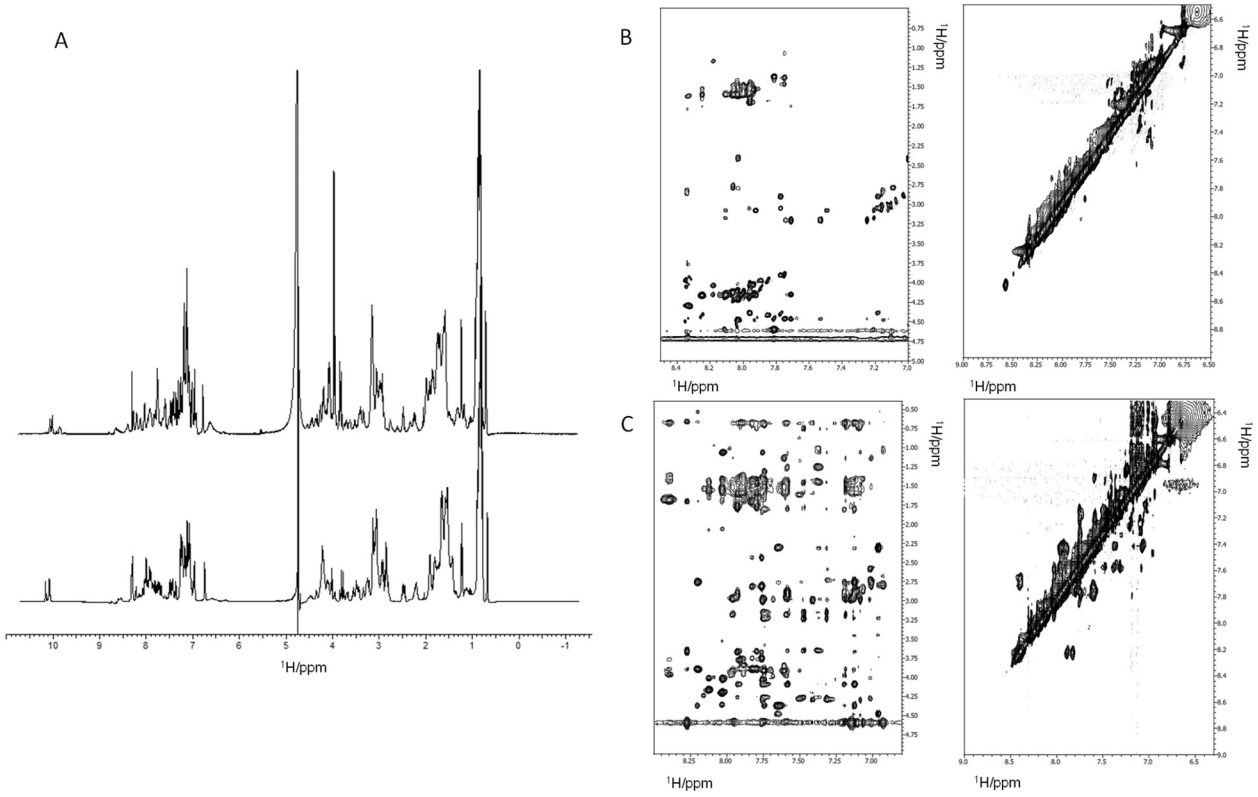

Fig. 5. NMR conformational analysis. A) Superposition ^{1}H NMR spectrum of GVF27 in water (upper) and in water/TFE mixture (lower). B) 2D [^{1}H, ^{1}H] NOESY spectrum of GVF27 in water at 298 K and pH 7.0 and C) in water/TFE mixture at 298 K and pH 7.0.

Table 3
Proton chemical shifts (ppm) of GVF27 in TFE-d3/H_2O (30:70) at 298 K.

Residue	NH	αH	βH	γH	Others
Gly1	7.97	3.70			
Val2	8.10	3.99	1.95	0.96	
Phe3	7.90	4.58	2.92		2,6H 7.32; 3,5H 7.24
Tyr4	7.58	4.48	2.67		2,6H 6.95; 3,5H 6.73
Pro5		4.32	2.13; 1.98	1.89	δCH_2 3. 45
Trp6	7.68	4.32			2H 7.23; 4H 7.57; 6H 7.20; 7H 7.52; NH 10.02
Arg7	8.03	4.09	1.74		δCH_2 2.84
Phe8	7.76	4.59	2.88		2,6H 7.22; 3,5H 7.34
Arg9	7.86	3.85	1.60; 1.48	1.62	δCH_2 2.95
Leu10	7.74	3.96	1.74	1.50	δCH_3 0.85
Leu11	8.37	3.93	1.73	1.45	δCH_3 0.91
Cys12	7.56	4.58	3.00		
Leu13	7.85	3.88	1.65	1.48	δCH_3 0.82
Leu14	7.53	4.08	1.83	1.54	δCH_3 0.93
Arg15	7.57	3.94	1.71		
Arg16	7.55	4.00	1.89	1.71	δCH_2 3.33
Trp17	7.26	4.36	3.24; 3.00		2H 7.13; 4H 7.35; 6H 7.11; 7H 7.22; NH 9.89
Leu18	7.72	3.97	1.58	1.40	δCH_3 0.90
Pro19		4.21	2.40; 2.24	1.88	δCH_2 3. 55
Arg20	8.08	4.13	1.65	1.48	δCH_2 3.03
Pro21		4.23	2.40; 2.19		δCH_2 3. 36
Arg22	7.88	4.27	1.79	1.54	δCH_2 3.06
Ala23	7.25	4.16	1.27		
Trp24	7.46	4.32	3.26; 3.19		2H 7.02; 4H 7.31; 6H 7.07; 7H 7.20; NH 9.99
Phe25		4.41	2.78; 2.64		2,6H 7.00; 3,5H 6.80
Ile26	7.45	4.02	1.67	1.20	γCH_3 0.93; δCH_3 0.78
Arg27	7.32	4.32	1.53;1.28		δCH_2 2.98

Table 4
CYANA structural statistic of GVF27 in TFE-d3/H_2O (30:70).

No. of the distance restraints	
Unambiguous NOE	267
Ambiguous NOE	91
Total NOE	358
Divided into	
Intra-residue NOE	119
Sequential NOE	88
Medium- and Long- range NOE	60
Residual NOE violations	
Number > 0.1°	± 1
Maximum, Å	0.16 ± 0.06
Residual angle violations	
Number > 2.0°	0 ± 0
Maximum, Å	0
R.m.s.d (Å) to a mean structure	
Backbone (residues (5–20)	0.19 ± 0.10
Heavy atoms (residues (5–20)	1.24 ± 0.15
Ramachandran plot residues (%)[b]	
In most favored regions	62.1
In additional allowed regions	27.3
In generously allowed regions	10.6
In disallowed regions	0.0

4. Discussion

Host defense peptides (HDPs) are important modulators in both mammalian and non-mammalian systems to prevent microbial colonization and tissue damage [52]. In mammals, such peptides constitute the major proportion (over 10% of total protein) among immune cells involved in immediate defense against aggressive microbes as well as in acute inflammatory reactions [53]. HDPs beneficial effects may encompass direct antimicrobial activity, binding to and inactivating endotoxins, such as LPS or LTA, which reduce the detrimental pro-inflammatory response, and one or more direct effects on cellular

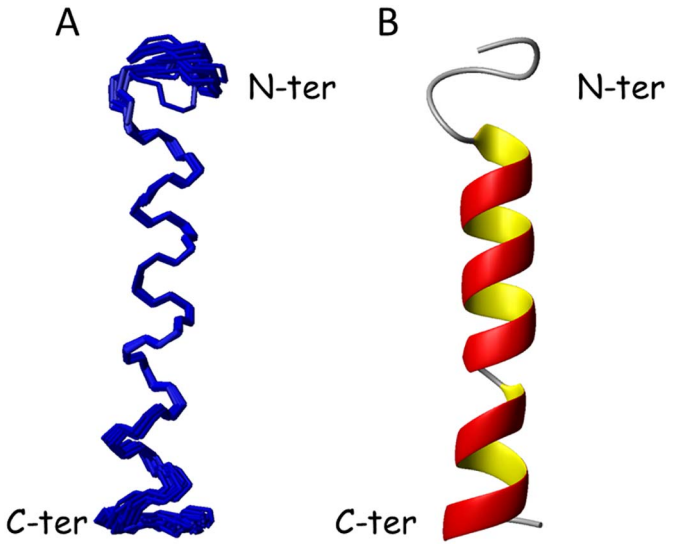

Fig. 6. NMR structures of GVF27 in TFE-d3/H_2O 30:70 mixture at 298 K A) Backbone superposition of the 20 energy-minimized structures and B) Ribbon model of a representative structure.

Table 5
Observed and calculated average hydrogen bond lengths for GVF27 in TFE-d3/H_2O (30:70).

Number	Residue	Atom	Number	Residue	Atom	Distance (Å)
7	Arg	HN	3	Phe	O	1.97
11	Leu	HN	7	Arg	O	2.20
13	Leu	HN	9	Arg	O	1.94
14	Leu	HN	10	Leu	O	1.92
22	Arg	HN	18	Leu	O	2.10
23	Ala	HN	19	Pro	O	1.99
24	Phe	HN	21	Pro	O	1.95

behaviors, such as enhanced migration and proliferation. The majority of HDPs share common biochemical features, including relatively small size, cationicity and amphipathicity in membrane-mimicking environments. These features allow them to selectively interact with and damage bacterial membranes.

A number of human proteins, whose primary functions are not necessarily related to host defense, contain HDPs hidden inside their sequence [54–55,40]. Our group has established a bioinformatic procedure (manuscript submitted) through which it is possible to identify host defense peptides in precursor protein sequences and predict their strain dependent antimicrobial propensities. By using this tool to analyze about 4000 human secreted proteins, a cryptic peptide has been identified in human 11-hydroxysteroid dehydrogenase-1 β-like (accession number UniProtKB: Q7Z5J1), here named GVF27, with potent antimicrobial activity (see Fig. S1).

The experiments described in this paper confirm that GVF27 peptide exhibits antibacterial activities, with MIC values comparable to that of a well studied cathelicidin, against a broad spectrum of both Gram-positive and -negative strains. Interestingly, its antibacterial properties are not limited to planktonic cells but are significant also on sessile bacteria forming biofilm. Indeed, here we provide evidences that GVF27 inhibits biofilm formation, as well as it is able to eradicate existing mature biofilm in a dose dependent manner. In addition, GVF27 is also able to induce a strong reduction of viable sessile bacterial cells. This suggests that our peptide presents affinity for biofilm components, presumably extracellular DNA and/or polysaccharides, but also retains its ability to attack bacterial membranes due to its amphipatic properties. This clearly confers to the peptide a relevant potential as an anti-biofilm agent alternative to conventional antibiotics, the latter almost totally ineffective against microbes encapsulated in biofilm.

A crucial point regarding the development of membranolytic antimicrobial therapeutics is that they must not destroy the membrane of mammalian cells. We showed here that, although endowed with antimicrobial activity, GVF27 displays virtually no hemolytic and cytotoxic activity on an assortment of murine and human cell lines. This implies that GVF27, probably due its net positive charge composition, has evident high membrane selectivity towards bacterial cells but not mammalian cells.

From a structural point of view, in agreement with the canonical properties of most HDPs, we verified by CD and NMR experiments that GVF27 is unstructured in aqueous buffer whereas it tends to assume a helical conformation in the presence of TFE. Moreover, NMR data clearly indicate that the spatial segregation of polar and apolar amino acids of GVF27 are on opposite faces oriented along the axis of a helical

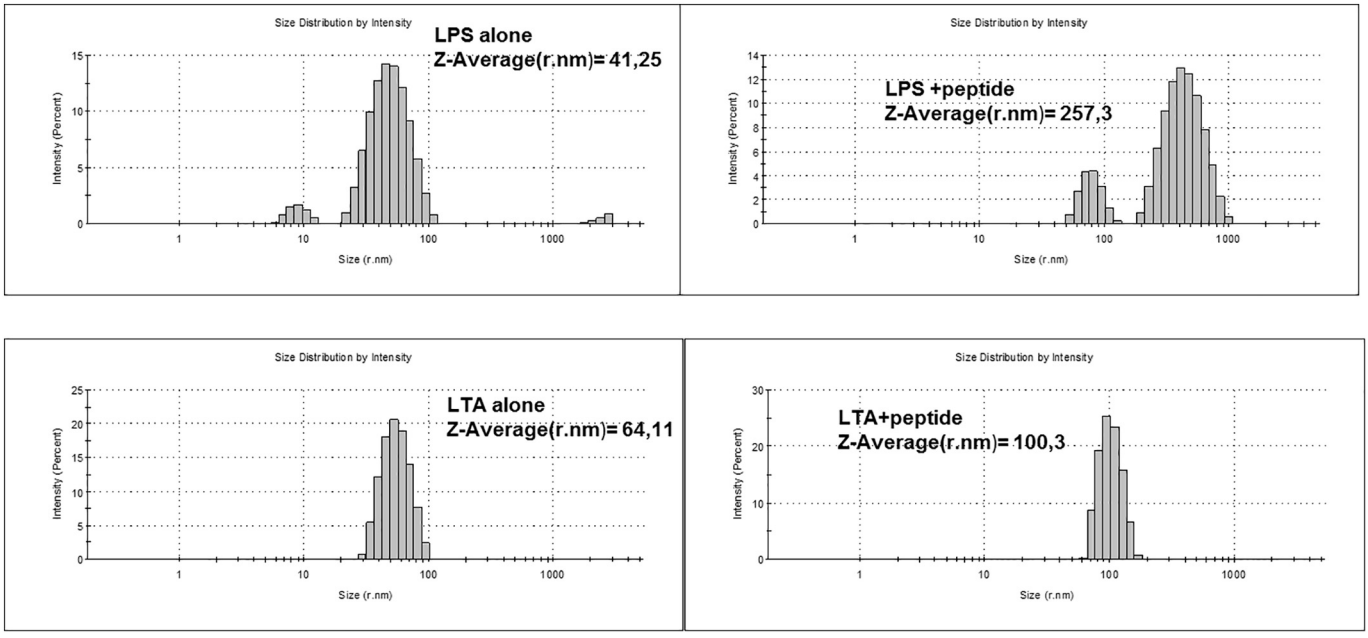

Fig. 7. Effect of GVF27 on the structural organization of LPS or LTA micelles. Light scattering of LPS from *P. aeruginosa* 10 (top) or LTA (bottom) before and after incubation with the peptide.

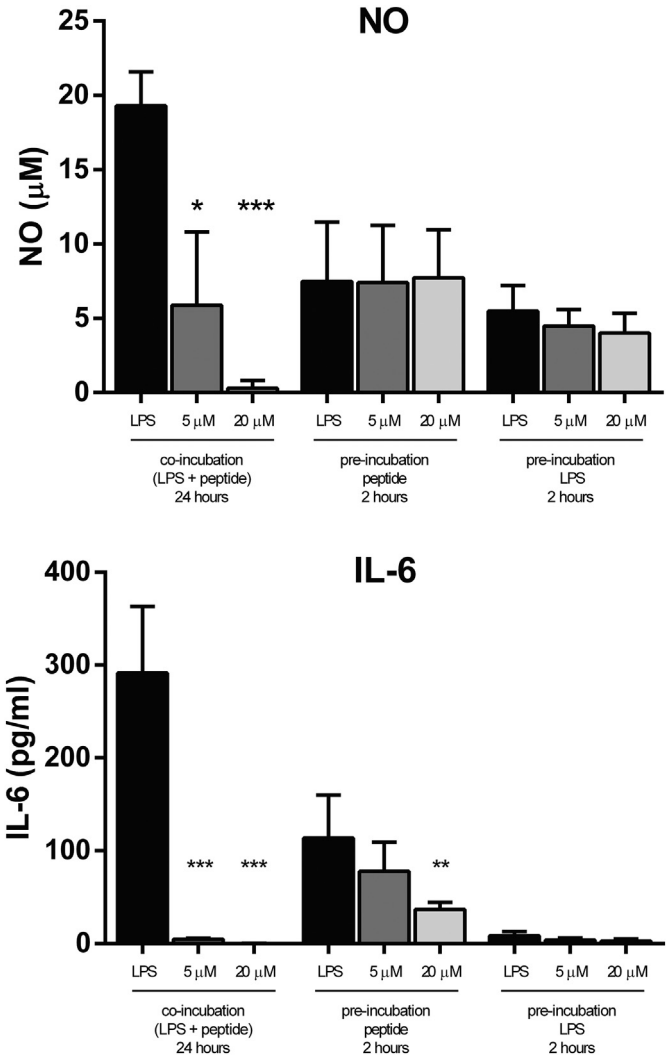

Fig. 8. (A) Effect of GVF27 on NO production in LPS induced mouse macrophages RAW 264.7. (B) Effect of GVF27 on IL-6 release in LPS induced mouse macrophages RAW 264.7 LPS extracted from *Salmonella minnesota* was assayed at a final concentration of 50 ng/mL (see Materials and methods section). All experiments were carried out for a total incubation time of 24 h.

structure. This would indicate that GFV27 is able to assume an optimal conformation to effectively promote strong membrane association.

Further tests by CD and light scattering have also allowed to highlight that the peptide is able to interact both with LPS and LTA, albeit in a less effective manner with the latter, thus suggesting that it can bind to the microbial surfaces via these wall determinants. The ability of GVF27 to interact with LPS has been also confirmed by different approaches, thanks to which it has been possible to show that the peptide is able to inhibit the pro-inflammatory response. Indeed, GVF27 strongly down-regulates the release of NO and the production of IL-6 both in LPS pre-treated murine macrophages cells and upon co-administration of the peptide and the endotoxin. Moreover, it is worth noting that in murine macrophages treated with GVF27 and then subjected to LPS, a decrease of both NO and IL-6 was still detectable, thus suggesting also a protecting action for the peptide. This opens an interesting scenario because GVF27 is a “hidden” peptide in a protein that, although not yet been characterized, could be constitutively present under physiological conditions and able to release, by induced proteolysis, a fragment containing GVF27 in response to pathogen invasion. Our hypothesis is substantiated by an *in silico* prediction of peptides obtainable as a result of hydrolysis, which was carried out on the isoforms in which we identified GVF27 by simulating hydrolysis mediated by neutrophil elastase. Indeed, as shown in Fig. S9, possible peptides released by hydrolysis are virtually superimposable to GVF27 and all have high antimicrobial scores, thus clearly supporting our idea that human proteins may fascinatingly be seen as active reservoirs of HDPs.

Finally, it seems very interesting the ability of GVF27 to attenuate LPS-induced pro-inflammatory response and its apparent ability to protect the cells by mitigating upstream the effects of infection. In both cases it seems plausible to hypothesize for GVF27 different targets.

In our opinion at least three mechanisms could be responsible for GVF27 immune-modulatory properties. First, GVF27 might modulate cellular response to pro-inflammatory mediators by acting as an endotoxin scavenger during initial steps of infection. In this case the peptide could bind to and neutralize the endotoxin directly. Second, GVF27 might reduce inflammatory dysfunction during immune response by interacting with membrane receptors, i.e. CD14, that then would activate down regulation of different pro-inflammatory pathways. Third, endogenous GVF27, or internalized from paracrine cells, may contribute to attenuation of the inflammatory response by interacting with intracellular targets. Based on these hypotheses and on the evidences described in this work, it is indisputable that the existence of cryptic HDPs implies that innate immunity is more complex than usually believed and that human proteome is an unexplored and essential source of bioactive agents.

In conclusion, GVF27 may offer several advantages compared to other antimicrobial agents,: (i) it is non-immunogenic given its human origin; (ii) specifically targets bacterial strains, (iii) is not hemolytic and contributes to enhance anti-inflammatory response without altering cell viability.

Thus, we confidentially believe that structural, immunomodulatory and antimicrobial data of GVF27 presented in this work, could serve as leads for the design of human-specific therapeutics.

Transparency document

The http://dx.doi.org/10.1016/j.bbagen.2017.04.009 associated with this article can be found, in online version.

Acknowledgments

We thank Rita Faella for her skillful technical assistance and drawing skills. This study was supported by the Italian Cystic Fibrosis Foundation (grant number 20/2014). We are deeply indebted to volunteers who devote many efforts in fundraising, in particular delegations from Palermo and Ragusa Vittoria Catania 2.

Appendix A. Supplementary data

Supplementary data to this article can be found online at http://dx.doi.org/10.1016/j.bbagen.2017.04.009.

References

[1] P. Bulet, R. Stöcklin, L. Menin, Anti-microbial peptides: from invertebrates to vertebrates, Immunol. Rev. 198 (2004) 169–184.
[2] J.P. Tam, S. Wang, K.H. Wong, W.L. Tan, Antimicrobial peptides from plants, Pharmaceuticals (Basel) 8 (4) (2015) 711–757.
[3] R.E. Hancock, E.F. Haney, E.E. Gill, The immunology of host defence peptides: beyond antimicrobial activity, Nat. Rev. Immunol. 16 (5) (2016) 321–343.
[4] F. Guilhelmelli, N. Vilela, P. Albuquerque, S. Lda Derengowski, I. Silva-Pereira, C.M. Kyaw, Antibiotic development challenges: the various mechanisms of action of antimicrobial peptides and of bacterial resistance, Front. Microbiol. 4 (2013) 353.
[5] D. Kraus, A. Peschel, Molecular mechanisms of bacterial resistance to antimicrobial peptides, Curr. Top. Microbiol. Immunol. 306 (2006) 231–250.
[6] D.I. Andersson, D. Hughes, J.Z. Kubicek-Sutherland, Mechanisms and consequences of bacterial resistance to antimicrobial peptides, Drug Resist. Updat. 26 (2016) 43–57.
[7] G. Diamond, N. Beckloff, A. Weinberg, K.O. Kisich, The roles of antimicrobial peptides in innate host defense, Curr. Pharm. Des. 15 (21) (2009) 2377–2392

(2009).
[8] M. Malmsten, Interactions of antimicrobial peptides with bacterial membranes and membrane components, Curr. Top. Med. Chem. 16 (1) (2016) 16–24.
[9] A. Bhunia, P.N. Domadia, J. Torres, K.J. Hallock, A. Ramamoorthy, S. Bhattacharjya, NMR structure of pardaxin, a pore-forming antimicrobial peptide, in lipopolysaccharide micelles: mechanism of outer membrane permeabilization, J. Biol. Chem. 285 (6) (2010) 3883–3895.
[10] P. Schmitt, R.D. Rosa, D. Destoumieux-Garzón, An intimate link between antimicrobial peptide sequence diversity and binding to essential components of bacterial membranes, Biochim. Biophys. Acta 1858 (5) (2016) 958–970.
[11] Y.R. Bommineni, G.H. Pham, L.T. Sunkara, M. Achanta, G. Zhang, Immune regulatory activities of fowlicidin-1, a cathelicidin host defense peptide, Mol. Immunol. 59 (1) (2014) 55–63.
[12] M.G. Scott, D.J. Davidson, M.R. Gold, D. Bowdish, R.E. Hancock, The human antimicrobial peptide LL-37 is a multifunctional modulator of innate immune responses, J. Immunol. 169 (7) (2002) 3883–3891.
[13] N. Mookherjee, K.L. Brown, D.M. Bowdish, S. Doria, R. Falsafi, K. Hokamp, F.M. Roche, R. Mu, G.H. Doho, J. Pistolic, J.P. Powers, J. Bryan, F.S. Brinkman, R.E. Hancock, Modulation of the TLR-mediated inflammatory response by the endogenous human host defense peptide LL-37, J. Immunol. 176 (4) (2006) 2455–2464.
[14] D. Bowdish, D.J. Davidson, D.P. Speert, R.E.W. Hancock, The human cationic peptide LL-37 induces activation of the extracellular signal-regulated kinase and p38 kinase pathways in primary human monocytes, J. Immunol. 172 (2004) 3758–3765.
[15] M.G. Scott, A.C. Vreugdenhil, W.A. Burman, R.E.W. Hancock, M.R. Gold, Cutting edge: cationic antimicrobial peptides block the binding of lipopolysaccharide (LPS) to LPS binding protein, J. Immunol. 164 (2000) 549–553.
[16] A. Giacometti, O. Cirioni, R. Ghiselli, F. Mocchegiani, F. Orlando, C. Silvestri, A. Bozzi, A. Di Giulio, C. Luzi, M.L. Mangoni, D. Barra, V. Saba, G. Scalise, A.C. Rinaldi, Interaction of antimicrobial peptide temporin L with lipopolysaccharide in vitro and in experimental rat models of septic shock caused by gram-negative bacteria, Antimicrob. Agents Chemother. 50 (7) (2006) 2478–2486.
[17] J. Agier, M. Efenberger, E. Brzezińska-Błaszczyk, Cathelicidin impact on inflammatory cells, Cent. Eur. J. Immunol. 40 (2) (2015) 225–235.
[18] A.L. Hilchie, K. Wuerth, R.E. Hancock, Immune modulation by multifaceted cationic host defense (antimicrobial) peptides, Nat. Chem. Biol. 9 (12) (2013) 761–768.
[19] N. Mookherjee, R.E. Hancock, Cationic host defence peptides: innate immune regulatory peptides as a novel approach for treating infections, Cell. Mol. Life Sci. 64 (7–8) (2007) 922–933.
[20] A. Zanfardino, E. Pizzo, A. Di Maro, M. Varcamonti, G. D'Alessio, The bactericidal action on *Escherichia coli* of ZF-RNase-3 is triggered by the suicidal action of the bacterium OmpT protease, FEBS J. 277 (8) (2010) 1921–1928.
[21] G. D'Alessio, Denatured bactericidal proteins: active per se, or reservoirs of active peptides? FEBS Lett. 585 (15) (2011) 2403–2404.
[22] P. Wang, L. Hu, G. Liu, N. Jiang, X. Chen, J. Xu, W. Zheng, L. Li, M. Tan, Z. Chen, H. Song, Y.D. Cai, K.C. Chou, Prediction of antimicrobial peptides based on sequence alignment and feature selection methods, PLoS One 6 (4) (Apr 13 2011) e18476.
[23] K. Pane, L. Durante, O. Crescenzi, V. Cafaro, E. Pizzo, M. Varcamonti, A. Zanfardino, V. Izzo, A. Di Donato, E. Notomista, Antimicrobial potency of cationic antimicrobial peptides can be predicted from their amino acid composition: application to the detection of "cryptic" antimicrobial peptides, J. Theor. Biol. 419 (Feb 17 2017) 254–265.
[24] R. Sukhija, P. Kakar, V. Mehta, J.L. Mehta, Enhanced 11beta-hydroxysteroid dehydrogenase activity, the metabolic syndrome, and systemic hypertension, Am. J. Cardiol. 98 (4) (2016) 544–548.
[25] Y. Kallberg, U. Oppermann, H. Jörnvall, B. Persson, Short-chain dehydrogenases/reductases (SDRs), Eur. J. Biochem. 269 (18) (Sep 2002) 4409–4417.
[26] C. Huang, B. Wan, B. Gao, S. Hexige, L. Yu, Isolation and characterization of novel human short-chain dehydrogenase/reductase SCDR10B which is highly expressed in the brain and acts as hydroxysteroid dehydrogenase, Acta Biochim. Pol. 56 (2) (2009) 279–289.
[27] Y. Xiao, H. Dai, Y.R. Bommineni, J.L. Soulages, Y.X. Gong, O. Prakash, G. Zhang, Structure-activity relationships of fowlicidin-1, a cathelicidin antimicrobial peptide in chicken, FEBS J. 273 (12) (Jun 2006) 2581–2593.
[28] I. Wiegand, K. Hilpert, R.E. Hancock, Agar and broth dilution methods to determine the minimal inhibitory concentration (MIC) of antimicrobial substances, Nat. Protoc. 3 (2) (2008) 163–175.
[29] R. Cooper, L. Jenkins, S. Hooper, Inhibition of biofilms of *Pseudomonas aeruginosa* by Medihoney in vitro, J. Wound Care 23 (3) (Mar 2014) 93–96.
[30] K.H. Park, Y.H. Nan, Y. Park, J.I. Kim, I.S. Park, K.S. Hahm, S.Y. Shin, Cell specificity, anti-inflammatory activity, and plausible bactericidal mechanism of designed Trp-rich model antimicrobial peptides, Biochim. Biophys. Acta 1788 (5) (2009) 1193–1203.
[31] S. Correale, C. Esposito, L. Pirone, L. Vitagliano, S. Di Gaetano, E. Pedone, A biophysical characterization of the folded domains of KCTD12: insights into interaction with the GABAB2 receptor, J. Mol. Recognit. 26 (10) (2013) 488–495.
[32] R. Del Giudice, A. Arciello, F. Itri, A. Merlino, M. Monti, M. Buonanno, A. Penco, D. Canetti, G. Petruk, S.M. Monti, A. Relini, P. Pucci, R. Piccoli, D.M. Monti, Protein conformational perturbations in hereditary amyloidosis: differential impact of single point mutations in ApoAI amyloidogenic variants, Biochim. Biophys. Acta 1860 (2) (2016) 434–444.
[33] M. Leone, P. Di Lello, O. Ohlenschläger, E.M. Pedone, S. Bartolucci, M. Rossi, B. Di Blasio, C. Pedone, M. Saviano, C. Isernia, R. Fattorusso, Solution structure and backbone dynamics of the K18G/R82E *Alicyclobacillus acidocaldarius* thioredoxin mutant: a molecular analysis of its reduced thermal stability, Biochemistry 43 (20) (2004) 6043–6058.
[34] P. Güntert, C. Mumenthaler, K. Wüthrich, Torsion angle dynamics for NMR structure calculation with the new program DYANA, J. Mol. Biol. 273 (1997) 283–298.
[35] R. Koradi, M. Billeter, K. Wüthrich, MOLMOL: a program for display and analysis of macromolecular structures, J. Mol. Graph. 14 (1) (Feb 1996) 51–55 (29-32).
[36] V.A. Schneider, M. Coorens, S.R. Ordonez, J.L. Tjeerdsma-van Bokhoven, G. Posthuma, A. van Dijk, H.P. Haagsman, E.J. Veldhuizen, Imaging the antimicrobial mechanism(s) of cathelicidin-2, Sci. Rep. 6 (2016) 32948.
[37] M. Coorens, M.R. Scheenstra, E.J. Veldhuizen, H.P. Haagsman, Interspecies cathelicidin comparison reveals divergence in antimicrobial activity, TLR modulation, chemokine induction and regulation of phagocytosis, Sci. Rep. 19 (2017) 7, http://dx.doi.org/10.1038/srep40874.
[38] E.J. Veldhuizen, V.A. Schneider, H. Agustiandari, A. van Dijk, J.L. Tjeerdsma-van Bokhoven, F.J. Bikker, H.P. Haagsman, Antimicrobial and immunomodulatory activities of PR-39 derived peptides, PLoS One 9 (4) (2014) e95939.
[39] N. Takei, N. Takahashi, T. Takayanagi, A. Ikeda, K. Hashimoto, M. Takagi, T. Hamada, E. Saitoh, A. Ochiai, T. Tanaka, M. Taniguchi, Antimicrobial activity and mechanism of action of a novel cationic α-helical dodecapeptide, a partial sequence of cyanate lyase from rice, Peptides 42 (2013) 55–62.
[40] D. Pletzer, S.R. Coleman, R.E. Hancock, Anti-biofilm peptides as a new weapon in antimicrobial warfare, Curr. Opin. Microbiol. 33 (2016) 35–40.
[41] A.I. Herrera, J.M. Tomich, O. Prakash, Membrane interacting peptides: a review, Curr. Protein Pept. Sci. 17 (8) (2016) 827–841.
[42] E. Notomista, A. Falanga, S. Fusco, L. Pirone, A. Zanfardino, S. Galdiero, M. Varcamonti, E. Pedone, P. Contursi, The identification of a novel *Sulfolobus islandicus* CAMP-like peptide points to archaeal microorganisms as cell factories for the production of antimicrobial molecules, Microb. Cell Factories 14 (2015) 126.
[43] D.S. Wishart, B.D. Sykes, Chemical shifts as a tool for structure determination, Methods Enzymol. 239 (1994) 363–392.
[44] K. Pane, V. Sgambati, A. Zanfardino, G. Smaldone, V. Cafaro, T. Angrisano, E. Pedone, S. Di Gaetano, D. Capasso, E.F. Haney, V. Izzo, M. Varcamonti, E. Notomista, R.E. Hancock, A. Di Donato, E. Pizzo, A new cryptic cationic antimicrobial peptide from human apolipoprotein E with antibacterial activity and immunomodulatory effects on human cells, FEBS J. 283 (11) (2016) 2115–2131.
[45] M.M. Domingues, R.G. Inácio, J.M. Raimundo, M. Martins, M.A. Castanho, N.C. Santos, Biophysical characterization of polymyxin B interaction with LPS aggregates and membrane model systems, Biopolymers 98 (4) (2012) 338–344.
[46] L. Heinbockel, L. Palacios-Chaves, C. Alexander, E. Rietschel, J. Behrends, W. Correa, S. Fukuoka, T. Gutsmann, A.J. Ulmer, K. Brandenburg, Mechanism of Hbγ-35-induced an increase in the activation of the human immune system by endotoxins, Innate Immun. 21 (3) (2015) 305–313.
[47] M. Hemshekhar, V. Anaparti, N. Mookherjee, Functions of cationic host defense peptides in immunity, Pharmaceuticals (Basel) 9 (3) (Jul 4 2016).
[48] T.J. Guzik, R. Korbut, T. Adamek-Guzik, Nitric oxide and superoxide in inflammation and immune regulation, J. Physiol. Pharmacol. 54 (4) (2003) 469–487.
[49] C.V. Suschek, O. Schnorr, V. Kolb-Bachofen, The role of iNOS in chronic inflammatory processes in vivo: is it damage-promoting, protective, or active at all? Curr. Mol. Med. 4 (7) (Nov 2003) 763–775.
[50] J. Scheller, A. Chalaris, D. Schmidt-Arras, S. Rose-John, The pro- and anti-inflammatory properties of the cytokine interleukin-6, Biochim. Biophys. Acta 1813 (5) (May 2011) 878–888.
[51] J.L. Ding, B. Ho, Endotoxin detection - from limulus amebocyte lysate to recombinant factor C, Subcell. Biochem. 53 (2010) 187–208.
[52] S.C. Mansour, O.M. Pena, R.E. Hancock, Host defense peptides: front-line immunomodulators, Trends Immunol. 35 (9) (Sep 2014) 443–450.
[53] T. Ganz, The role of antimicrobial peptides in innate immunity, Integr. Comp. Biol. 43 (2) (Apr 2003) 300–304.
[54] P. Papareddy, M. Kalle, G. Kasetty, M. Mörgelin, V. Rydengård, B. Albiger, K. Lundqvist, M. Malmsten, A. Schmidtchen, C-terminal peptides of tissue factor pathway inhibitor are novel host defense molecules, J. Biol. Chem. 285 (36) (Sep 3 2010) 28387–28398.
[55] E. Andersson, V. Rydengard, A. Sonesson, M. Morgelin, L. Bjorck, A. Schmidtchen, Antimicrobial activities of heparin-binding peptides, Eur. J. Biochem. 271 (2004) 1219–1226.